# Micromagnetic Phase Transitions and Spin Wave Excitations in a Ferromagnetic Stripe

Matthieu Bailleul,* Dominik Olligs,† and Claude Fermon

*Service de physique de l'état condensé, DRECAM/DSM CEA Saclay, Orme des merisiers, 91191 Gif sur Yvette, France.*

(Received 20 March 2003; published 26 September 2003)

Magnetic excitations of micrometer-wide ferromagnetic stripes subjected to a transverse applied field have been measured between 1 and 20 GHz . The complexity of the observed response is attributed to the spatially nonuniform equilibrium spin distribution. This one is modeled analytically and numerically, which allows one to distinguish two micromagnetic phases governing the ground state. The nucleation-related phase transitions are evidenced by soft modes, while the different observed resonances are attributed to spin wave modes localized in the two phases and at their interface.

DOI: 10.1103/PhysRevLett.91.137204 PACS numbers: 75.60.–d, 75.30.Ds, 75.40.–s, 76.50.+g

The varied spin distributions adopted by finite-size ferromagnets have stimulated a large number of studies in the past 15 years [1]. A convenient way to describe their magnetization process is to gather the possible configurations into micromagnetic phases [1,2] and determine the related phase transitions. However, the magnetic volume involved in these transitions may be very small, which makes it difficult to probe them using conventional magnetometry and magnetic imaging. In an alternative way, linear response measurements may be used to determine the elementary excitations (spin wave modes [3]) which, in turn, reflect the structure of the equilibrium. Such high-frequency dynamics studies were recently carried out by several groups, but most of these were analyzed assuming quasiuniform equilibrium spin distributions [3,4] and the nonuniform dynamics, described mainly in the case of transversely magnetized stripes [5–7], were not systematically correlated with the structure of the ground state. Also, up to now, as written by Aharoni [8], "in spite of the similarity, resonance modes have been studied without paying much attention to the relation to the nucleation problem."

To investigate this issue, we have used ferromagnetic stripes on which a magnetic field $\mathbf{H}_0$ is applied in the transverse direction [$\hat{x}$ axis in Fig. 1(a)]. This hinders the flux-closure tendency of the dipole-dipole interaction, resulting in the formation of magnetic surface and/or volume charges which, in turn, produce long-range dipole fields. Contrary to the ellipsoid case, where a uniform magnetization produces a uniform dipole field, the resulting equilibrium is nonuniform [curling of the magnetization close to the edges [9,10], see Fig. 1(a)]. The linear response around this equilibrium state has been probed using a microwave microantenna technique we developed recently [11,12]. A continuous 30 nm permalloy ($Ni_{80}Fe_{20}$) film is first deposited on a glass substrate by e-beam evaporation. Then, it is patterned into an array of 3 $\mu$m wide 3 $\mu$m spaced stripes by optical lithography and normal incidence ion beam etching. After deposition of a 100 nm thick $Si_3N_4$ insulating film, a two conductor coplanar microantenna is fabricated above the stripes [see Fig. 1(b)]. This antenna is shorted at one end and connected, at the other end, to a vector network analyzer, which allows one to measure the real and imaginary parts of the input impedance [13]. As the coupling of the antenna to the stripes is purely inductive, the spin response is evaluated by a suitable extraction of the self-inductance, the spin eigenmodes appearing as resonances of this response function. Contrary to conventional ferromagnetic resonance, this technique is broadband, which allows one to follow the changes in micromagnetic structure induced by changing the applied field. The strong localization of the pumping field (on a region of a few micrometers around the antenna) results in a high filling factor, which gives a good sensitivity. But it also results in the excitation of modes being nonuniform along the $\hat{y}$ direction ($k_y \simeq 0.2\ \mu\mathrm{m}^{-1}$ for the antenna used here [11]). In the case of our stripes, this is of importance only when the excited eigenmode is quite uniform along $\hat{x}$ (i.e., when $k_x < k_y$) and can then be accounted for using the magnetostatic wave theory [11].

Low field measurements are reported on Fig. 1(c), which shows the absorption signal (imaginary part of the self-inductance) as a function of the microwave frequency and applied transverse field. In the high-field regime, field-sweep spectra are recorded for different frequencies [inset of Fig. 1(d)] and the positions of the observed resonances are collected together [main frame of Fig. 1(d)]. From a phenomenological point of view, note first the two soft-mode inflections: around 100 mT for the low frequency mode and around 12 mT for the intense, high-frequency resonance. Note also the existence of four modes immediately below the intense resonance.

Analyzing this response requires one to understand the ground state itself. For a first glance, let us assume the stripes are (i) thin enough so that the equilibrium magnetization $\mathbf{M}$ lies in the plane and does not vary along the thickness, (ii) wide enough so that exchange effects can be ignored, (iii) long enough so that the equilibrium spin distribution is uniform along $\hat{y}$. This allows one to write the equilibrium equation of micromagnetics [1] in a purely one-dimensional form:

  

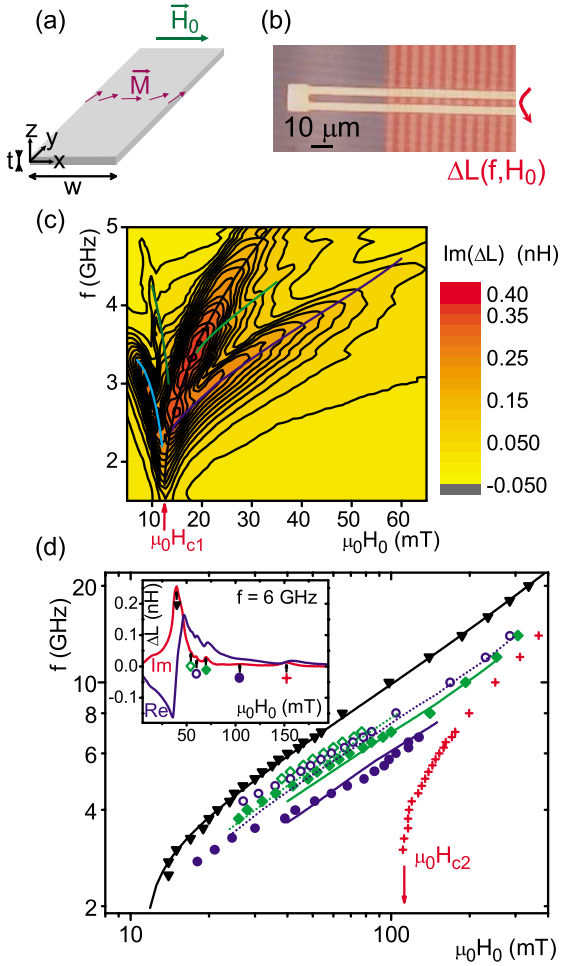


FIG. 1 (color). Microwave response of an array of transversely magnetized permalloy stripes. (a) Sketch of the equilibrium configuration. (b) Microphotograph showing part of the array of 3 μm wide stripes (pink vertical strips) and the shorted end of the microantenna (white horizontal strips). (c) Color plot of the imaginary part of the self-inductance (absorption) in the low-field regime. Lines are guides for the eyes. (d) Location of the resonances observed on the high-field spectra (inset: typical spectrum at 6 GHz). In the text, we refer to the high-frequency (triangle), the low-frequency (cross) and the four intermediate resonances (other symbols). The lines are deduced from calculations detailed at the end of this letter. Black line: center mode. Solid and dotted, blue and green lines: interface related standing-wave modes (mode numbers from 1 to 4, from bottom to top).

$$\mathbf{H}_{\text{eff}}(x) = \lambda(x)\mathbf{M}(x), \tag{1}$$

where $\lambda(x)$ is a Lagrange multiplier, accounting for the constraint $\mathbf{M}^2 = M_s^2$ and $\mathbf{H}_{\text{eff}}$ is the equilibrium effective field. In this approximation $\mathbf{H}_{\text{eff}}(x) = \mathbf{H}_0 + \mathbf{H}_d(x)$, $\mathbf{H}_d$ being the dipole field. Because of symmetry, $\mathbf{H}_{\text{eff}}$ lies along the $\hat{x}$ axis. The $\hat{y}$ component of Eq. (1) is therefore $\lambda(x)M_y(x) = 0$. Following Schäfer and DeSimone [14], we will distinguish two kinds of solutions: a field-expulsion phase [$\lambda(x) = 0 \Rightarrow H_{\text{eff}}(x) = 0$] and a field-penetration phase which, here, is saturated [$\lambda(x) \neq 0 \Rightarrow M_y(x) = 0$]. In our case, field expulsion is primarily edge related: in order to save the energy cost of edge magnetic charges, the magnetization curls into the $\hat{y}$ axis. This creates volume magnetic charges $\rho(x) = -\frac{dM_x}{dx}$, whose magnetostatic field is able to compensate exactly $\mathbf{H}_0$. In order to calculate $\rho(x)$ Bryant and Suhl [15] have identified this problem as that of a conducting strip, where electrostatic charges expel any applied electric field . Two specific features arise, however, in the ferromagnetic case due to the vector nature of the magnetization. First, the sign of $M_y(x) \neq 0$ is not fixed by micromagnetics, i.e., the $(xz)$ mirror symmetry is broken in the field-expulsion phase. Second, the amount of charge is limited: as the total rotation in each half of the stripe should not exceed 90°, we get $|\int_0^x \rho(x')dx'| \leq M_s$. Therefore, a total expulsion of the magnetic field [left panel of Fig. 2(a)] is possible only for low enough applied fields. Above $H_{c1} = \frac{t}{w}M_s$, the high-symmetry saturated phase nucleates at the center of the stripes [right panel of Fig. 2(a)]. To support

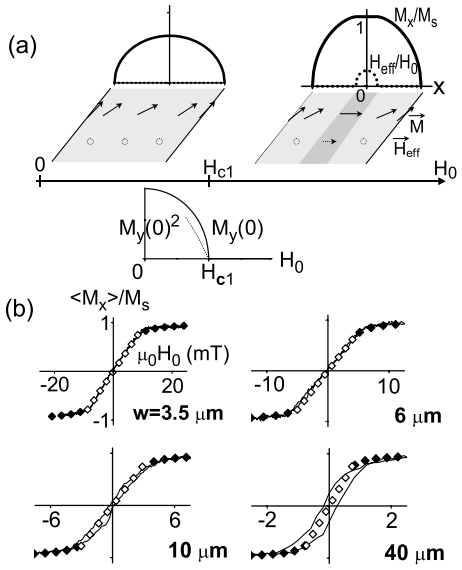


FIG. 2. Equilibrium magnetic configuration in the low field regime. (a) Calculated transverse magnetization and equilibrium field profiles below and above the nucleation of the saturated phase (left: $H_0 = 0.67H_{c1}$; right: $H_0 = 1.1H_{c1}$). The expulsion phase is sketched in light gray, the saturated one in dark gray. Calculations according to Ref. [15]; in the mixed phase, the interaction between the two field-expulsion areas was taken into account by a mean-field coefficient adjusted so that they coalesce at the critical point [12]. The order parameter (longitudinal component of the magnetization at the center of the stripe) is reported in the inset. (b) Average transverse magnetization for arrays of stripes with different width $w$. The Kerr-effect measurements are reported as continuous lines. The dots are deduced from the calculation described above (open dots: expulsion phase, solid dots: mixed expulsion-saturation phase).

this simple magnetostatic approach, we measured the transverse magnetization curves for several arrays of stripes with different widths. The measurements are reported as lines in Fig. 2(b), together with the predictions of the magnetostatic approach (dots). The agreement, holding over a decade of stripe width, is very satisfying.

When the applied field is increased further, the low-symmetry areas get very narrow (their width, evaluated as $\frac{\pi M_s}{H_0} t$ [15], is of the order of 200 nm for our stripes under a 50 mT field), with the result that the exchange interaction, being short range, cannot be neglected anymore. To investigate this effect, we have performed micromagnetic simulations, using the software OOMMF [16]. The stripe cross section is divided into $5 \times 5\ \mathrm{nm}^2$ cells and the spin distribution is obtained by relaxation from a fictitious saturated state. The saturation magnetization is $\mu_0 M_s = 1.13$ T (deduced from polarized neutron reflectivity measurements), the exchange stiffness is assumed to be $A = 10^{-11}\ \mathrm{J\,m^{-1}}$ and the magnetocrystalline anisotropy is set to zero, in agreement with magnetization loops measured on the continuous film. Compared to the predictions of the dipolar approach, the simulated magnetization and effective field profiles confirm the existence of field-free and saturation regions [Fig. 3(a)]. However, their interface is not perfectly sharp. This is attributed to the nonzero $\hat{y}$ component of the exchange field ( $\propto \frac{d^2 M_y}{dx^2}$ ) which, inserted in Eq. (1), allows the order parameter $M_y$ to be nonzero even in the field-penetration area. In order to monitor directly the symmetry properties of the ground state for higher fields (i.e., far above $\mu_0 H_{c1}$, which is of the order of 11 mT for our 3 μm stripes), we have thus followed the cross-sectional spin distribution very close to the edge. This latter was assumed to have a 30° slope, in order to account for the faceting effect associated with normal incidence ion beam etching [10,17]. Even though corner effects [18] forbid a perfect saturation of the stripe [see vector field in Fig. 3(b)], one actually observes an annihilation of the low-symmetry area. This occurs at the top corner [see gray scale on Fig. 3(b)], for a field $\mu_0 H_{c2} = 129$ mT.

The two nucleation-annihilation events described above are accompanied by a local symmetry breaking. They should therefore be phase transitions of the second order. This is illustrated by plotting the corresponding order parameters [insets of Figs. 2(a) and 3(b)]: both of them vanish at the critical points with a critical exponent $\beta = \frac{1}{2}$, as predicted by the Landau theory [19]. For such critical points, one also expects the curvature of the free energy along a special path in the configuration space to vanish, which causes the vanishing of the corresponding eigenfrequency [20]. This fact can be used in two ways. First, the soft-mode inflections on the microwave response can be used to evaluate the critical fields; note the agreement between the measured values (12 and 100 mT) and the calculated values (11 and 129 mT). Second, the corresponding eigenmodes should look

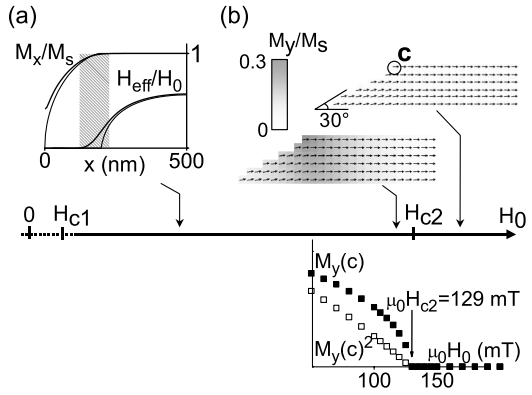


FIG. 3. Simulated equilibrium magnetic configuration in the high-field regime. (a) Transverse magnetization and equilibrium field profiles on the half-width of a 1 μm wide stripe. Thin and thick lines are deduced from magnetostatic theory and micromagnetic simulation, respectively. The shaded area is the interface region between the two phases. Parameters are $w = 1$ μm, $\mu_0 H_0 = 50$ mT. (b) Simulated spin configuration in the cross section of a 3 μm wide stripe for $\mu_0 H_0 = 125$ mT (bottom) and 130 mT (top). The edge region has been zoomed in. The vector plot and the gray scale show respectively the $(xz)$ projection and the $\hat{y}$ component of the magnetization field. The edge slope has been set to 30°. The bottom inset shows the order parameter (longitudinal component of the magnetization at the top corner cell).

very similar to the nucleation modes [Figs. 2(a) and 3(b)], which allows us to distinguish between two modes located mostly in the center of the stripe and on the edges [respectively, triangles and crosses in Fig. 1(d)].

The corresponding eigenfrequencies are calculated using the linearized Landau-Lifshitz equation [1]:

$$i\omega \mathbf{m} = \gamma \mu_0 \mathbf{H}_{\mathrm{eff}} \times \mathbf{m} - \gamma \mu_0 \mathbf{M} \times \mathbf{h}, \qquad (2)$$

where $\mathbf{m}$ ($\mathbf{h}$) is the dynamic part of the magnetization (effective field), $\omega$ is the angular frequency, and $\gamma$ is the gyromagnetic ratio (here, $\frac{\gamma}{2\pi} = 29\ \mathrm{GHz\,T^{-1}}$ deduced from the microwave response of the continuous film). In order to estimate the resonance frequency of the center mode, one uses the dipolar one-dimensional approximation seen above: the dynamic effective field is separated into a local out-of-plane component [$h_z(x) = -m_z(x)$] and a long-range in-plane component [$h_x(x)$, which is a functional of $m_x(x)$]. Now, note that the spins which precess in the saturated area neither produce nor feel any in-plane dipole field ($\mathbf{M} \parallel \hat{x} \Rightarrow m_x = 0$ at first order and $\mathbf{M} \times h_x \hat{\mathbf{x}} = 0$). This mode is therefore decoupled from the field-expulsion phase. Its frequency can be estimated as that of the uniform parallel resonance under a field which is the equilibrium field in the center of the stripe, the nonuniformity of the pumping field being taken into account using the magnetostatic wave theory [Eq. (2) of Ref. [11] with $k = k_y \simeq 0.2\ \mu\mathrm{m}^{-1}$]. The obtained frequency [black line in Fig. 1(d)] is in very good

agreement with the position of the high-frequency resonance.

In this one-dimensional dipolar approximation, the in-plane restoring torque at the interface between the two phases vanishes [$\mathbf{H}_{\text{eff}} = 0$ and $\mathbf{M} \times h_x \hat{\mathbf{x}} = 0$ in Eq. (2)], which results in a vanishing resonance frequency. However, taking into account exchange and finite thickness slightly modifies the ground state [Fig. 3(a)] and also creates a dynamic coupling with neighboring regions. This can be accounted for using a WKB-like approach: as in Refs. [5–7] which deal with similar systems, the eigenmodes are approximated locally as plane spin waves propagating along $\hat{x}$. The propagation path is bounded by two turning points on which waves are reflected back: one is located in the saturated area, a few hundreds of nanometers from the interface region [6] and the other is set at the physical edge of the stripe. Indeed, contrary to Refs. [6,7], we think that the wave is also able to propagate in the field-expulsion area. The distributions of $\mathbf{M}$ and $\mathbf{H}_{\text{eff}}$, needed to calculate the local spin wave dispersions, are deduced from micromagnetic simulations similar to that of Fig. 3(a). The frequencies calculated in this way for the first four standing-wave modes are represented in Fig. 1(d) as blue and green lines. They are in reasonable agreement with the position of the four intermediate modes. The wave vector profiles for these modes (not shown) confirm their strong localization around the interface region: the maximum wave vector, reached in the middle of the interface region, is about 30 $\mu\text{m}^{-1}$ for an applied field of about 70 mT [12]. Of practical importance are the relative amplitudes of the observed peaks: while at least two different modes contribute significantly to the response below $2H_{c1}$ [Fig. 1(c)], the resonance of the saturated phase is by far the most intense one above $5H_{c1}$ [Fig. 1(d)]. This illustrates directly the transition between highly nonuniform dynamics, as observed, for example, in vortex structures [21], and quasiuniform dynamics, as observed in recent precessional switching experiments [4].

In summary, we have studied transversely magnetized ferromagnetic stripes, which, due to finite-size effects, exhibit complex nonuniform equilibrium spin distributions. Those distributions were described theoretically in terms of two micromagnetic phases. The microwave response, directly influenced by those phases, was used to probe the magnetization process. Whereas our analysis was strongly simplified by the one-dimensional translation invariance of our system, the obtained results could apply, at least qualitatively, to other systems involving "edge curling walls": edges of hard ferromagnets [18,22] or submicrometer dots at remanence [2,20].

The authors wish to thank S. O. Demokritov and B. Hillebrands for providing the permalloy film and for useful discussions, F. Ott for performing the polarized neutrons reflectivity measurements, and O. Klein for his help. This work is supported by the European Union through Contract No. M2EMS (IST-2001-34594).

*Present address: Institut für Experimentelle und Angewandte Physik, Universität Regensburg, 93040 Regensburg, Germany.
Electronic address: matthieu.bailleul@physik.uni-regensburg.de
†Present address: Leibniz Institut für Festkörper- und Werkstoffforschung, Helmholtzstrasse 20, 01069 Dresden, Germany.

[1] A. Hubert and R. Schäfer, *Magnetic Domains* (Springer, Berlin, 1998).
[2] R. P. Cowburn and M. E. Welland, Appl. Phys. Lett. **72**, 2041 (1998).
[3] *Spin Dynamics in Confined Magnetic Structures*, edited by B. Hillebrands and K. E. Ounadjela (Springer, Berlin, 2001), Vol. 1.
[4] W. K. Hiebert., G. E. Ballentine, and M. R. Freeman, Phys. Rev. B **65**, 140404 (2002); T. Gerrits, H. A. M. van den Berg, J. Hohlfeld, and T. Rasing, Nature (London) **418**, 509 (2002); S. Kaka and S. E. Russek, Appl. Phys. Lett. **80**, 2958 (2002); H. W. Schumacher *et al.*, Phys. Rev. Lett. **90**, 017201 (2003).
[5] P. H. Bryant, J. F. Smyth, S. Schultz, and D. R. Fredkin, Phys. Rev. B **47**, 11255 (1993).
[6] J. Jorzick *et al.*, Phys. Rev. Lett. **88**, 047204 (2002).
[7] J. P. Park *et al.*, Phys. Rev. Lett. **89**, 277201 (2002); C. Bayer, S. O. Demokritov, B. Hillebrands, and A. N. Slavin, Appl. Phys. Lett. **82**, 607 (2003).
[8] A. Aharoni, *Introduction to the Theory of Ferromagnetism* (Clarendon Press, Oxford, 1996).
[9] R. M. Hornreich, J. Appl. Phys. **34**, 1071 (1963).
[10] R. Mattheis, K. Ramstöck, and J. McCord, IEEE Trans. Magn. **33**, 3993 (1997).
[11] M. Bailleul, D. Olligs, C. Fermon, and S. O. Demokritov, Europhys. Lett. **56**, 741 (2001).
[12] M. Bailleul, Ph.D. thesis, Ecole Polytechnique, 2002.
[13] Coaxial standards are used for calibration; the coplanar-coaxial transition is modeled as a section of 50 Ω transmission line.
[14] R. Schäfer and A. DeSimone, IEEE Trans. Magn. **38**, 2391 (2002).
[15] P. Bryant and H. Suhl, Appl. Phys. Lett. **54**, 2224 (1989).
[16] www.nist.gov.
[17] R. E. Lee, J. Vac. Sci. Technol. **18**, 164 (1979).
[18] W. Rave, K. Ramstöck, and A. Hubert, J. Magn. Magn. Mater. **183**, 329 (1998).
[19] L. D. Landau and E. Lifshitz, *Course of Theoretical Physics* (Pergamon, Oxford, 1969), Vol. 5.
[20] O. Gérardin, Ph.D. thesis, Université de Brest, 2001.
[21] Y. Acremann *et al.*, Science **290**, 492 (2000); V. Novosad *et al.*, Phys. Rev. B **66**, 052407 (2002); J. P. Park *et al.*, Phys. Rev. B **67**, 020403(R) (2003).
[22] O. Fruchart, B. Kevorkian and J. C. Toussaint, Phys. Rev. B **63**, 174418 (2001).